

### Selection of optimum parameters

For the purpose of succinctness, only the optimisation of MSIS-PET(IR) in HG mode for the Agilent 5100 will be discussed in this section. Similar contour plots of blank-subtracted signal intensities and Mg II/ Mg I ratios trends were observed for 35 elemental lines, resulting in a simple compromise for optimal settings. The similarity of optimal conditions for different analytes agrees with previous work in ICPMS in which one sampling position provided optimal sensitivity for practically all elements.<sup>1</sup> Due to instrumental limits, the “optimised” conditions are sometimes located at a maximum value. For instance, RF power was set to the maximum of 1.5 kW on the Agilent 5100. This follows from the literature, as a robust plasma is achieved when the RF power is at least 1400 W,<sup>2</sup> and higher RF power increases robustness.<sup>3</sup>

The high RF power combined with 0.6 L min<sup>-1</sup> carrier gas directly correlates to the findings of Novotny *et al.*<sup>4</sup> that a lower carrier gas flow is necessary to reduce the amount of aerosol (and in doing so, reduce the solvent loading), and to increase the residence time. This also allows the aerosol to be more thoroughly vaporized by the IR heater prior to beginning atomization in the lower region of the plasma. As only the aerosol exiting the spray chamber is heated, 2 mL min<sup>-1</sup> sample loading can be handled.

Whereas the Mg II/ Mg I ratio peaked at both 100 °C and 250 °C IR temperature (Fig. S2), 100 °C provided the highest signal intensities for all analytes and minimised the risk of melting the upper areas of the torch casing (i.e. the gas inlets) due to the convective nature of the rope heater.

In lateral view, univariate optimisation of plasma observation height was also done following optimisation of all other parameters. 2 mm was chosen for PET(IR) because the Mg II/ Mg I ratio decreased at higher observation heights (Fig. S3), as previously reported.<sup>4,5</sup>

### References

- 1 S. Liu and D. Beauchemin, *Spectrochim. Acta B*, 2006, **61**, 157 – 163.
- 2 J. M. Mermet, *Anal. Chim. Acta*, 1991, **250**, 85 – 94.
- 3 X. Romero, E. Poussel and J. M. Mermet, *Spectrochim. Acta B*, 1997, **52**, 487 – 493.
- 4 I. Novotny, J. C. Farinas, J. L. Wan, E. Poussel and J. M. Mermet, *Spectrochim. Acta B*, 1996, **51**, 1517 – 1526.
- 5 M.T. Cicerone, P.B. Farnsworth, *Spectrochim. Acta B*, 1989, **44**, 897-907.

**Table S1** Optimised conditions for MSIS-ICPOES and MSIS-PET(IR)-ICPOES (lateral view ARCOS) in each of dual and HG modes

Condition	Dual		HG	
	No PET	PET(IR)	No PET	PET(IR)
RF power (kW)	1.45	1.45	1.45	1.45
Plasma gas (L min <sup>-1</sup> )	12	14	12	12
Auxiliary gas (L min <sup>-1</sup> )	1.0	1.0	1.0	1.0
Nebulizer gas (L min <sup>-1</sup> )	0.7	1.0	0.8	0.8
Sample uptake (mL min <sup>-1</sup> )	2.0	2.0	2.0	2.0
IR temperature (°C)	---	175	---	175
Plasma observation height (mm)	11	11	11	11

**Table S2** Selected sensitivities and detection limits measured on ARCOS with MSIS operated in dual mode

Element line (nm)	Sensitivity (cps per $\mu\text{g L}^{-1}$ )			Detection limit ( $\mu\text{g L}^{-1}$ )		
	MSIS-PET <sup>7</sup>	MSIS-PET(IR)	MSIS	MSIS-PET <sup>7</sup>	MSIS-PET(IR)	MSIS
As I 189.042	280	280	510	0.2	0.1	0.2
Be I 234.861	990	740	1400	0.2	0.1	0.1
Bi I 223.061	220	340	590	0.5	0.08	0.2
Cd II 214.439	410	79	450	0.5	0.4	0.3
Co II 228.615	160	44	130	0.7	1	2
Cr II 267.716	60	24	60	2	1	2
Cu II 224.700	40	12	37	3	3	5
Fe II 238.204	110	55	160	8	1	1
Mn II 257.610	310	180	420	0.3	0.2	0.3
Ni II 231.604	70	21	64	3	2	2
Pb II 220.353	13	4.3	15	8	9	9
V II 292.464	50	220	470	1	0.2	0.8
Zn II 206.200	160	36	180	0.6	1	0.5

**Table S3:** Detection Limits ( $\mu\text{g L}^{-1}$ ) with Agilent 5100 for MSIS in dual mode with and without PET(IR) compared to pneumatic nebulisation

Element Line (nm)	PN		MSIS		MSIS-PET(IR)	
	Lateral	Axial	Lateral	Axial	Lateral	Axial
Al II 167.019	7	20	2	3	2	1
As I 189.042	30	50	2	0.4	2	0.6
Be I 234.861	0.7	0.1	0.5	0.4	0.6	0.2
Be II 313.042	0.1	0.06	0.03	0.8	0.03	0.03
Be II 313.107	0.2	0.06	0.1	0.07	0.05	0.06
Bi I 223.061	60	30	2	0.6	2	0.7
Cd II 214.439	0.6	2	0.7	0.6	0.7	0.3
Co II 228.615	8	3	3	2	6	1
Cr II 267.716	3	2	3	2	2	1
Cu II 224.700	20	7	10	4	10	4
Cu I 324.754	4	2	6	3	9	0.9
Fe II 238.204	3	2	2	1	4	1
Ge I 265.117	50	30	4	0.8	3	0.8
Hg I 184.887	4	6	0.3	0.2	0.2	0.07
K I 766.491	200	4	n.d.*	20	n.d.	6
Li I 670.783	10	0.1	10	0.1	10	0.1
Mg II 280.270	0.3	0.1	0.3	0.2	0.2	0.08
Mg I 285.213	7	1	4	0.5	4	1
Mn II 257.610	1	0.3	0.7	0.2	0.4	0.3
Mo II 202.032	10	9	20	3	9	2
Ni II 231.604	20	5	10	2	10	4
P I 177.434	60	90	30	10	20	8
Pb II 220.353	20	6	10	3	10	4
S I 180.669	100	70	0.04	0.02	0.03	0.02
Sb I 217.582	50	30	1	0.6	2	0.6
Se I 196.026	30	20	n.d.	n.d.	10	5
Si I 251.611	30	20	30	40	30	7
Sr II 421.552	0.2	0.06	0.3	0.08	0.3	0.1
Ti II 334.941	2	0.3	1	0.3	1	0.5
V II 292.464	1	0.3	4	3	4	1
Y II 371.029	0.9	0.3	0.8	0.4	1	0.3
Zn II 206.200	8	10	6	2	4	1
Zn I 213.857	2	2	1	0.8	2	0.6
Zr II 339.198	5	0.7	2	0.9	3	2

\* n.d. = not detected

**Table S4:** Detection Limits ( $\mu\text{g L}^{-1}$ ) with Agilent 5100 for MSIS in HG mode with and without PET(IR) and ratio of detection limits

Element Line (nm)	MSIS		MSIS-PET(IR)		MSIS/MSIS-PET(IR)	
	Lateral	Axial	Lateral	Axial	Lateral	Axial
As I 189.042	1	0.2	0.8	0.3	1	0.7
Be I 234.861	300	90	30	4	9	20
Be II 313.042	20	10	2	0.4	10	30
Be II 313.107	60	20	7	2	8	10
Bi I 223.061	0.9	0.3	0.8	0.3	1	1
Cd II 214.439	n.d.*	n.d.	2	0.1	---	---
Ge I 265.117	2	0.4	2	0.5	1	0.8
Hg I 184.887	0.2	0.04	0.1	0.07	2	0.6
Pb II 220.353	n.d.	n.d.	n.d.	80	---	---
Sb I 217.582	1	0.3	0.8	0.2	1	2
Se I 196.026	n.d.	n.d.	3	2	---	---

\* n.d. = not detected

**Table S5:** Detection Limits ( $\mu\text{g L}^{-1}$ ) with Agilent 5100 for MSIS in nebulisation mode with and without PET(IR) and ratio of detection limits

Element Line (nm)	MSIS		MSIS-PET(IR)		MSIS/MSIS-PET(IR)	
	Lateral	Axial	Lateral	Axial	Lateral	Axial
Al II 167.019	3	2	3	1	1	2
As I 189.042	50	20	30	10	2	2
Be II 313.042	0.2	0.07	0.06	0.2	3	0.4
Bi I 223.061	80	20	60	10	1	2
Cd II 214.439	1	0.3	0.9	0.2	1	2
Co II 228.615	8	1	4	1	2	1
Cr II 267.716	7	1	3	1	2	1
Cu II 224.700	20	5	10	6	2	0.8
Cu I 324.754	20	3	5	2	4	2
Fe II 238.204	10	2	2	2	5	1
Ge I 265.117	200	30	80	30	2	1
Hg I 184.887	0.5	0.2	0.3	0.1	2	2
K I 766.491	n.d.*	20	100	20	---	1
Li I 670.783	20	0.6	60	0.3	0.3	2
Mg II 280.270	0.8	0.2	0.3	0.08	3	3
Mg I 285.213	10	0.8	6	0.9	2	0.9
Mn II 257.610	1	0.4	0.5	0.4	2	1
Mo II 202.032	30	3	8	2	4	2
Ni II 231.604	20	5	8	3	3	2
P I 177.434	30	20	30	10	1	2
Pb II 220.353	30	5	10	7	3	0.7
S I 180.669	200	50	80	30	2	2
Sb I 217.582	100	30	70	20	1	2
Se I 196.026	70	10	30	10	2	1
Si I 251.611	40	8	20	7	2	1
Sr II 421.552	0.7	0.08	0.6	0.2	1	0.4
Ti II 334.941	3	1	2	0.8	2	1
V II 292.464	20	2	6	6	3	0.3
Y II 371.029	3	0.5	1	0.5	3	1
Zn II 206.200	6	2	3	2	2	1
Zn I 213.857	6	1	2	1	3	1
Zr II 339.198	10	3	5	3	2	1

\* n.d. = not detected

**Table S8:** Instrumental precision (% relative standard deviation for 100ppb, n=10) with Agilent 5100 for MSIS in dual mode with and without PET(IR) compared to pneumatic nebulisation

Element Line (nm)	PN		MSIS		MSIS-PET(IR)	
	Lateral	Axial	Lateral	Axial	Lateral	Axial
Al II 167.019	1.7	1.4	3	1.6	1.9	1.8
As I 189.042	2	1.5	1.6	1.5	1.2	1.8
Be I 234.861	0.93	1.1	1	1.6	0.85	0.3
Be II 313.042	0.87	0.41	1.1	1.5	2.1	1
Be II 313.107	0.93	0.46	1.1	1.5	1.9	1.1
Bi I 223.061	7	3.7	1.6	2.9	0.41	3.8
Cd II 214.439	0.85	0.7	0.89	1.5	0.29	0.61
Co II 228.615	0.32	0.61	1.7	2.3	0.7	2.5
Cr II 267.716	1.3	1.4	1.1	1.6	1.3	0.26
Cu II 224.700	0.83	1.2	6.8	1.9	5.6	2.8
Cu I 324.754	1.5	0.98	1.3	2	1.1	0.95
Eu II 420.505	0.8	1.4	2.1	5.7	2.2	2.1
Fe II 238.204	0.7	0.54	1.3	1.3	1.4	0.49
Ga I 294.364	2.4	1.2	9.6	3.4	15	3.9
Ge I 265.117	5	1.3	4.2	2.5	2	3.3
Hg I 184.887	5.3	6	1.6	2.3	1.1	8.1
In II 230.606	5.8	2.2	11	7.7	18	9.3
K I 766.491	1.3	1.5	3.8	9.6	3.5	5.1
La II 408.672	0.78	0.78	2.1	5.2	3.6	3.4
Li I 670.783	1	0.35	1.2	1.7	0.99	1.5
Mg II 280.270	0.52	0.29	2.4	5.9	3.5	5.2
Mg I 285.213	0.57	0.73	1.6	3.7	4.3	4.8
Mn II 257.610	0.52	0.91	1.3	1.5	0.72	0.99
Mo II 202.032	0.79	0.8	3.2	1.7	3.3	1.5
Ni II 231.604	0.92	0.84	2.5	1.7	3	3.1
P I 177.434	2	4.4	17	7.1	10	7.4
Pb II 220.353	2	0.96	1.7	1.7	5	2.6
S I 180.669	3.7	3.7	1.1	1.2	1	0.69
Sb I 217.582	4.7	2.2	3	2.6	1.6	4.9
Se I 196.026	2.5	1.5	6.1	6.8	3	3.3
Si I 251.611	1.4	0.82	4.2	0.8	6.4	3.2
Sr II 421.552	1.3	0.65	2.6	4.6	1.4	1.4
Ti II 334.941	0.65	1.2	0.79	2.4	1.2	1.6
V II 292.464	0.57	1	1.2	0.82	3.7	1.1
Y II 371.029	0.56	0.47	1.1	1.6	1.4	0.87
Zn II 206.200	0.74	0.69	2.8	1.6	1.6	0.74
Zn I 213.857	0.64	0.69	1.4	1.2	1	0.67
Zr II 339.198	0.54	0.33	3.6	1.6	1.7	0.58

**Table S9:** Instrumental precision (% relative standard deviation for 100ppb, n=10) with Agilent 5100 for MSIS in HG mode with and without PET(IR) compared to pneumatic nebulisation

Element Line (nm)	PN		MSIS		MSIS-PET(IR)	
	Lateral	Axial	Lateral	Axial	Lateral	Axial
As I 189.042	2	1.5	2.4	2.1	1.7	0.79
Be I 234.861	0.93	1.1	16	15	15	4.3
Be II 313.042	0.87	0.41	34	10	7.3	1
Be II 313.107	0.93	0.46	15	7.9	5.3	1.4
Bi I 223.061	7	3.7	1.5	3	2.6	1.1
Cd II 214.439	0.85	0.7	13	10	3.7	1.8
Co II 228.615	0.32	0.61	20	13	11	21
Ge I 265.117	5	1.3	5.3	1.7	1.5	1.4
Hg I 184.887	5.3	6	1.5	1.5	1.4	6.1
Pb II 220.353	2	0.96	23	16	24	43
Sb I 217.582	4.7	2.2	0.93	2	0.77	0.32
Se I 196.026	2.5	1.5	5.1	6.6	0.79	3.9

**Table S10:** Instrumental precision (% relative standard deviation for 100ppb, n=5) with Agilent 5100 for MSIS in nebulisation mode with and without PET(IR) compared to pneumatic nebulisation

Element Line (nm)	PN		MSIS		MSIS-PET(IR)	
	Lateral	Axial	Lateral	Axial	Lateral	Axial
Al II 167.019	1.7	1.4	2.3	3.2	1.7	1.5
As I 189.042	2	1.5	7.9	9.1	6.7	6.6
Be II 313.042	0.87	0.41	3.1	1.7	1.2	0.32
Bi I 223.061	7	3.7	31	8	9.8	8.1
Cd II 214.439	0.85	0.7	2.4	1.9	1.7	0.81
Co II 228.615	0.32	0.61	6.4	2.6	2.3	0.49
Cr II 267.716	1.3	1.4	3.2	2.1	1.7	0.49
Cu II 224.700	0.83	1.2	5.6	3.5	6.1	3.1
Cu I 324.754	1.5	0.98	1.9	1.6	2.4	0.68
Eu II 420.505	0.8	1.4	5.6	1.7	4.3	0.74
Fe II 238.204	0.7	0.54	3	2.3	2.7	0.78
Ga I 294.364	2.4	1.2	24	4.3	13	3.9
Ge I 265.117	5	1.3	25	7.2	7.7	5.8
Hg I 184.887	5.3	6	1.2	5.2	0.95	4.5
In II 230.606	5.8	2.2	22	10	35	13
K I 766.491	1.3	1.5	n/a	2.5	1.8	6.1
La II 408.672	0.78	0.78	5	2.9	3	1.3
Li I 670.783	1	0.35	1.2	3.6	0.37	1.7
Mg II 280.270	0.52	0.29	2.5	1.8	1.1	0.66
Mg I 285.213	0.57	0.73	3.5	1.6	1.2	0.84
Mn II 257.610	0.52	0.91	2.7	1.5	1.5	0.32
Mo II 202.032	0.79	0.8	4.5	1.6	2.8	2.4
Ni II 231.604	0.92	0.84	7.7	1.3	3.5	1.3
P I 177.434	2	4.4	11	5.4	6.3	2.3
Pb II 220.353	2	0.96	9.3	3.9	7.8	1.3
S I 180.669	3.7	3.7	16	15	21	20
Sb I 217.582	4.7	2.2	22	10	12	11
Se I 196.026	2.5	1.5	8.5	2.5	9.3	4.1
Si I 251.611	1.4	0.82	7.5	2.1	18	2
Sr II 421.552	1.3	0.65	2.3	1.4	1.9	0.56
Ti II 334.941	0.65	1.2	2	1.6	1.1	0.97
V II 292.464	0.57	1	4.4	1.2	2.7	0.97
Y II 371.029	0.56	0.47	2.9	1.6	1.7	0.54
Zn II 206.200	0.74	0.69	2.5	1.5	4.3	0.72
Zn I 213.857	0.64	0.69	2.6	3.4	1.9	0.61
Zr II 339.198	0.54	0.33	6.2	2.4	4.2	0.54

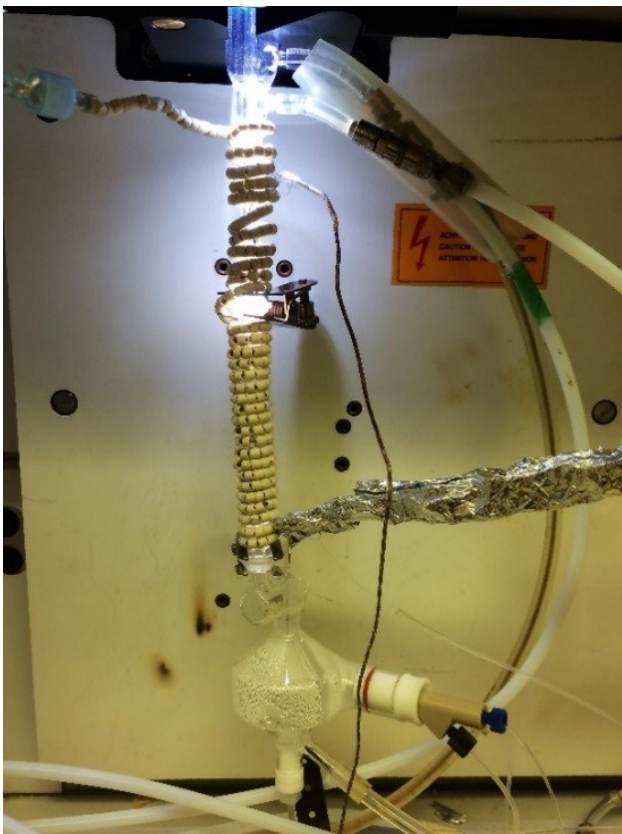


**Fig S1.** MSIS-PET(IR) on the SPECTRO ARCOS, heating the 8-cm PET and the bottom 7 cm of the torch

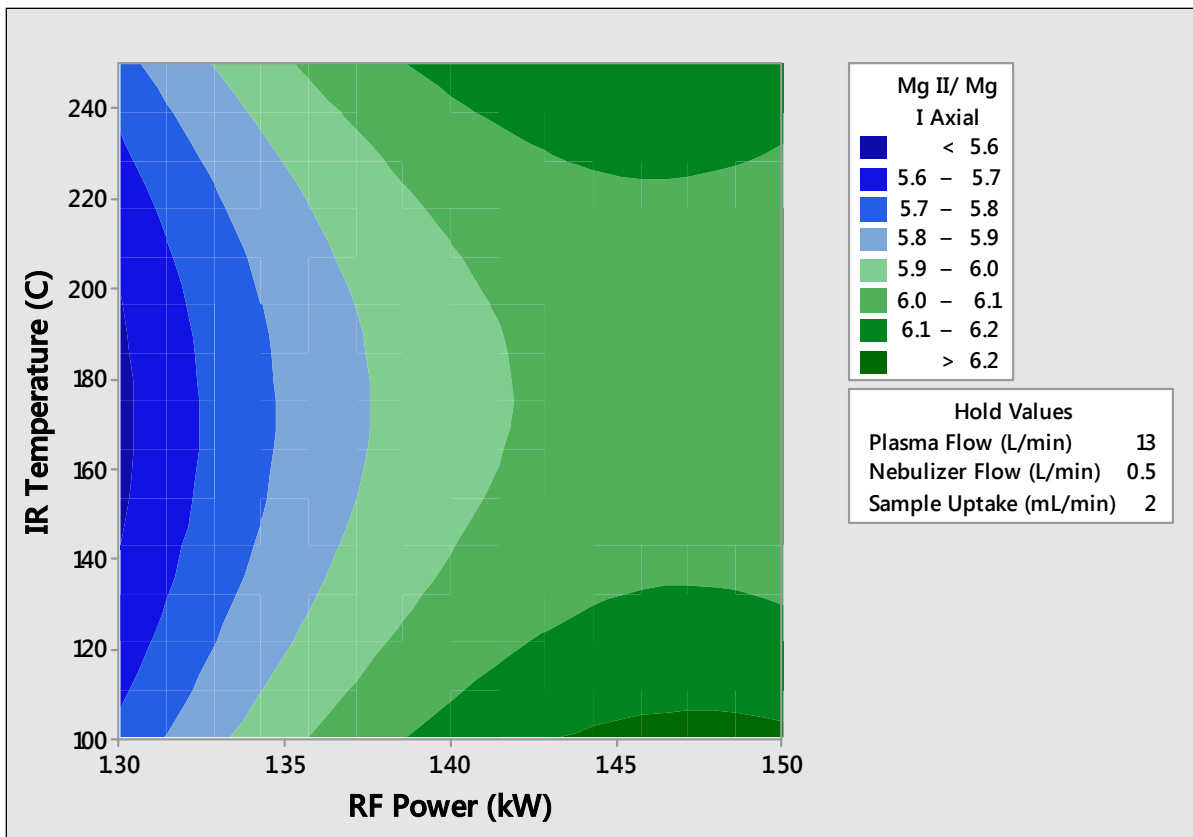


**Fig S2.** Contour plot of the  $Mg\text{ II}/Mg\text{ I}$  ratio at different IR temperatures and RF powers with MSIS-PET(IR) on the Agilent 5100 in axial view during multivariate optimisation in HG mode

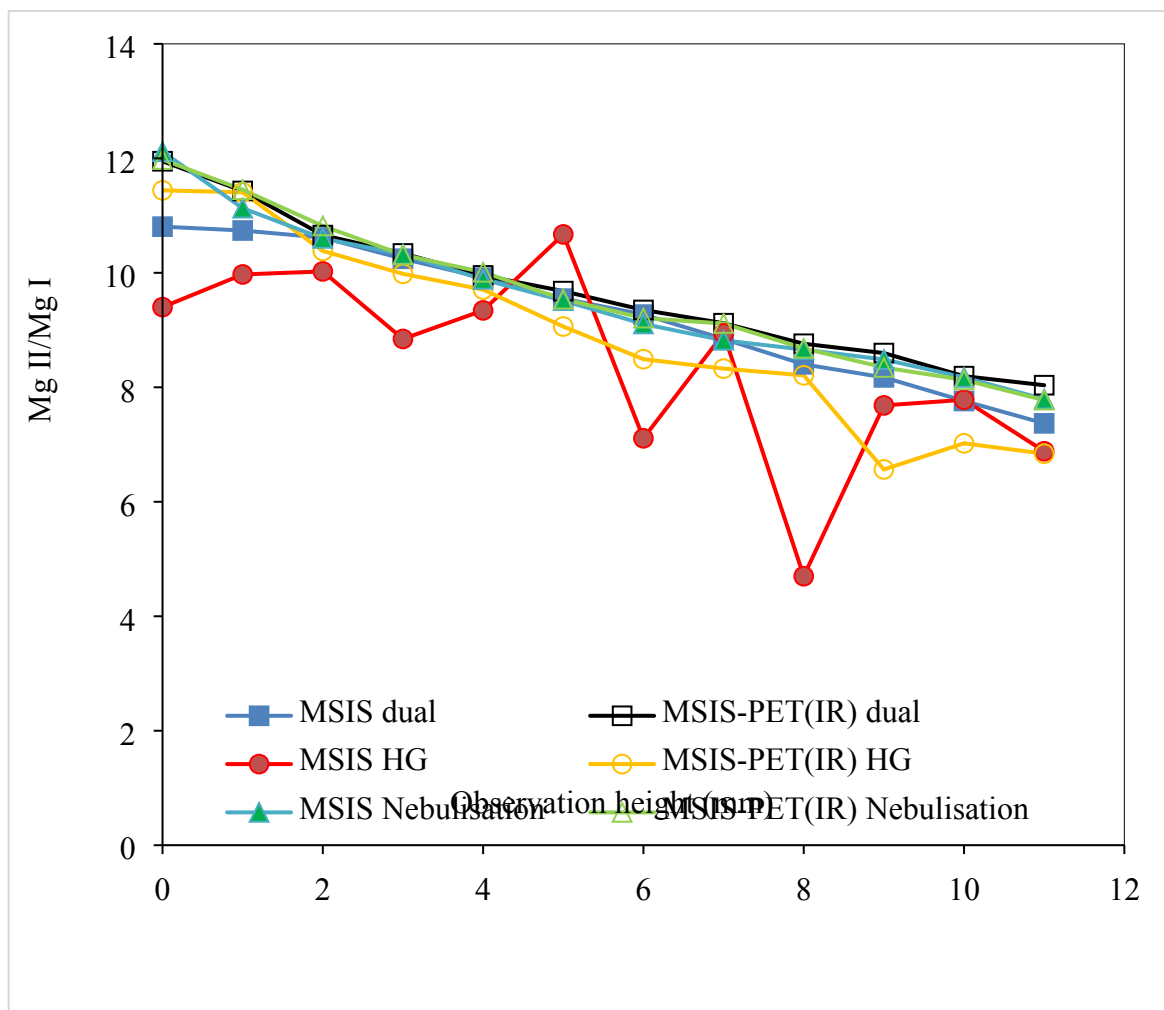


**Fig S3.** Effect of observation height on the Mg II/Mg I ratio on the Agilent 5100 with the MSIS in different operation modes, with and without PET(IR)

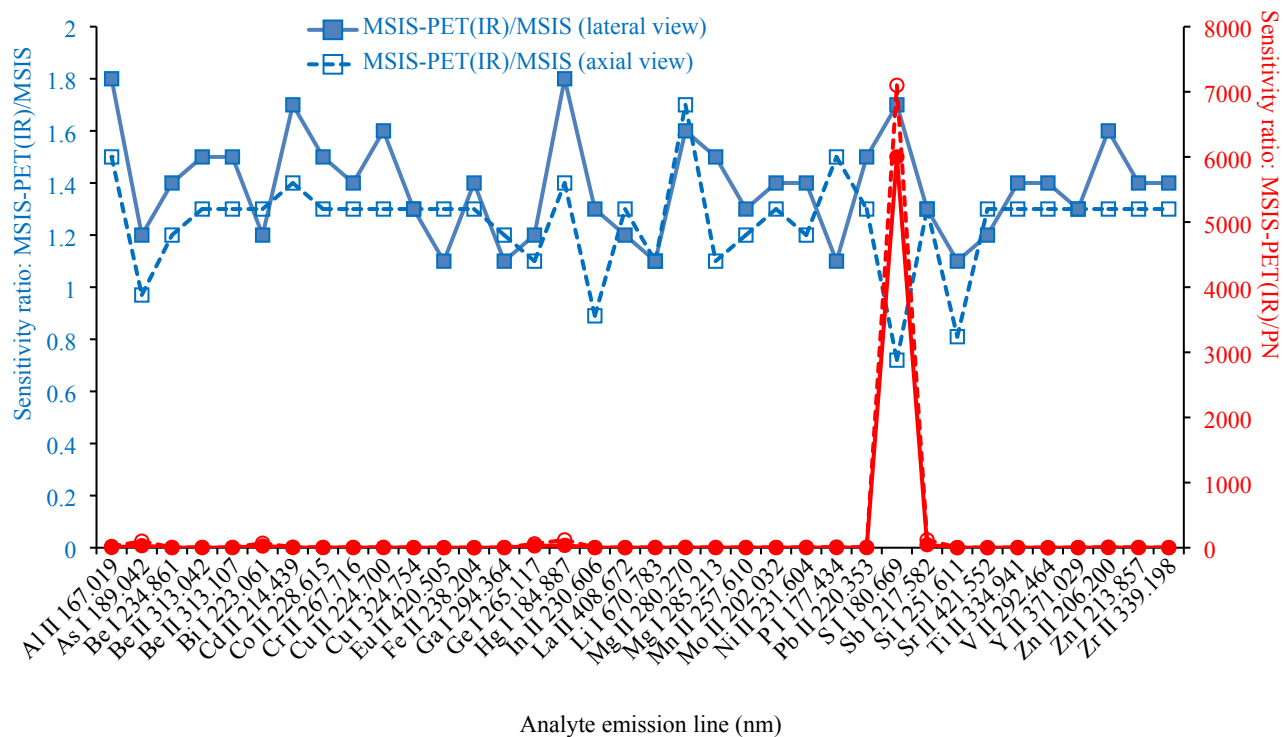


**Fig S4.** Sensitivity ratio with MSIS-PET(IR) in dual mode over regular MSIS in dual mode or PN; a ratio above 1 indicates improvement with MSIS-PET(IR). Note the log scale used to compare MSIS-PET(IR) to PN.

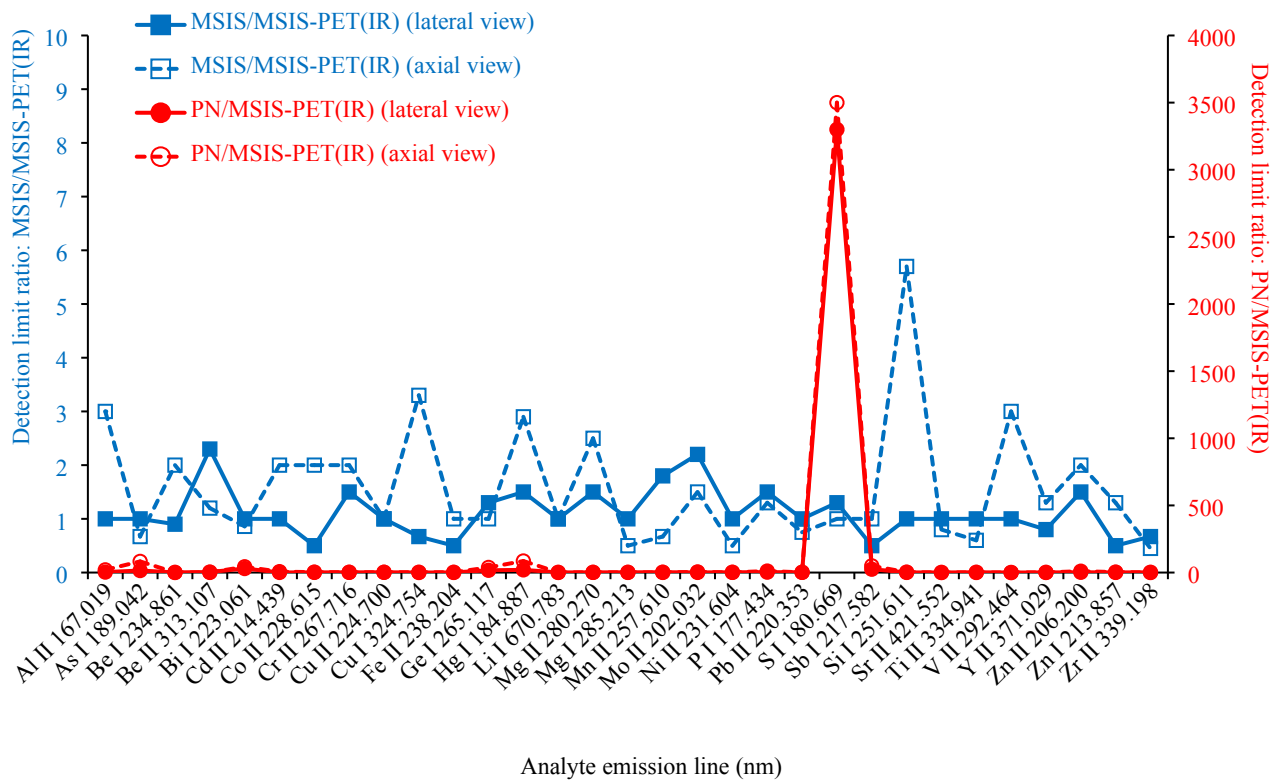


**Fig S5.** Detection limit ratio with regular MSIS in dual mode or PN over MSIS-PET(IR) in dual mode; a ratio above 1 indicates improvement with MSIS-PET(IR). Note the log scale used to compare MSIS-PET(IR) to PN.